Geodetic deformations in the Central-Southern Apennines (Italy) from repeated GPS surveys

Enrico Serpelloni ([1]), **Marco Anzidei** ([2]), **Paolo Baldi** ([1]), **Giuseppe Casula** ([2]), **Alessandro Galvani** ([2]), **Arianna Pesci** ([2]) **and Federica Riguzzi** ([2])

([1]) *Dipartimento di Fisica, Università di Bologna, Italy*

([2]) *Istituto Nazionale di Geofisica e Vulcanologia, Roma, Italy*

Abstract

We computed the horizontal strain rate field for a sector of the Central-Southern Apennines (Italy) from GPS data collected during yearly repeated campaigns performed from 1994 to 2000 on the GeoModAp (Geodynamic Modeling of the Apennines) geodetic network. Site velocities were obtained starting from the daily coordinates and covariance solutions, using a Kalman filter approach. The residual velocity field with respect to a Eurasian fixed reference frame shows two different prevalent motion trends, NE-ward for the eastern sector of the network and NW-ward for the western one. The mean strain rate tensor, obtained from a least square inversion method, shows a significant extensional deformation (1.2×10^{-8} strain/yr) normal to the Apennine chain, in agreement with seismological and neotectonic data. On the basis of the network dimension, of about 250 km, this value gives a well constrained estimate of about 3.0 ± 0.2 mm/yr of the extensional velocity oriented N55E, normal to the chain axis. Our results show a transition of the strain rate field from about N-S compression in the Tyrrhenian side to about NE-SW extension toward the Adriatic, which depicts a more complex deformation pattern.

Key words *geodesy – GPS – Central-Southern Apennines – strain rate – seismotectonic*

1. Introduction

The measure of the space and time pattern of tectonic strains by modern geodesy, based on GPS surveys performed over geodetic networks devoted to geophysical purpose, can quantify parameters directly linked to potential seismic activity even on still unknown seismogenetic structures. Geodetic measurements of crustal deformation can also provide direct tests of geodynamic models (Ward, 1994a,b). Even with this great potential, GPS is only beginning to play a major role in the study of crustal deformation in the Central Mediterranean area. In Italy, and in particular in Central and Southern Apennines, the number of permanent GPS stations is still too limited to provide a satisfactory description of the highly heterogeneous strain field which seems to affect this zone, as suggested by geological and seismological observations. Thus, the use of non continuous but denser GPS networks is still fundamental for geophysical research in the above zone.

This work describes and discusses the results obtained during the time span 1994-2000 by repeated GPS campaigns performed in Central-Southern Apennines. This region was fre-

Mailing address: Dr. Marco Anzidei, Istituto Nazionale di Geofisica e Vulcanologia, Via di Vigna Murata 605, 00143 Roma, Italy; e-mail: anzidei@ingv.it

quently subjected to large earthquakes in the past and it is still undergoing relatively high deformations rates (Anderson and Jackson, 1987; Jackson and McKenzie, 1988; Westaway, 1992; Bernardini and Gasperini, 1994; Kiratzi, 1994; Pondrelli *et al.*, 1995; Selvaggi, 1998; Hustand and England, 1999; Anzidei *et al.*, 2001; Viti *et al.*, 2001). Moreover, the Central-Southern Apennines may represents an exciting study area for applying a multidisciplinary approach to seismic hazard estimate, since in this region detailed studies have been already performed using different geophysical techniques, such as paleoseismology (Valensise and Pantosti, 2001 and references within), historical and instrumental seismology and macroseismic studies (Gasperini *et al.*, 1999).

2. Geodynamic and geological overview

The Mediterranean region is characterized by a complex mosaic of microplates, moving one with respect to the other to accommodate the interaction between Africa/Arabia and Eurasia. Crustal fragmentation and deformation are evidenced by the high seismic and volcanic activity extending from the Azores triple junction to Anatolia (Dewey *et al.*, 1989; Mantovani *et al.*, 1997a,b, 2000a,b). Along this complex margin the tectonic setting is highly heterogeneous with particular regard to the Italian region (fig. 1). In this context, the Apenninic belt represents a post-collisional Neogene segment of the Mediterranean African verging mountain system, where compression and extension have coexisted from late Tortonian to Quaternary times (Patacca and Scandone, 1989; Hippolyte *et al.*, 1994). In this belt subduction is still active beneath the Calabrian arc (Amato and Montone, 1997; Chiarabba and Amato, 1997; Lucente *et al.*, 1999). The Central-Southern Apennines consist of a pile of thrust sheets forming a complex duplex system in a tectonic stack of rock units derived from different Mesozoic-Paleogene sedimentary basins and shelves, orogenically transported over the flexured southwestern margin of the Apulia foreland. The western part of the chain is formed by Mesozoic and Cenozoic limestone massifs with peaks reaching 2000 m, while the front units of the chain are made of pelagic sedimentary formations, similar in age. East of the chain, the foredeep basin is filled with Plio-Quaternary sediments and was produced by the sinking of the Apulia foreland whose Mesozoic limestones crop out only in the Gargano area. The geodynamic setting of the chain displays a complex temporal evolution and the last orogenic phase occurred from the Late Miocene to the early Quaternary (Philip, 1987; Patacca *et al.*, 1990; Roure *et al.*, 1991). The analysis of focal mechanisms for recent earthquakes indicates dominant normal and strike-slip movements (Gasparini *et al.*, 1985; Frepoli *et al.*, 1996; Mantovani *et al.*, 1997b; Frepoli and Amato, 2000; Viti *et al.*, 2001). Analysis of fault slip data sets (Hippolyte *et al.*, 1994, 1995) from Quaternary geological units provides evidence for a recent change of strain fields (Early-Middle Pleistocene) that corresponds to a major change in the geodynamic setting of this zone (Cinque *et al.*, 1993; Pantosti *et al.*, 1993a; Hippolyte *et al.*, 1994, 1995; Mantovani *et al.*, 1997b; Valensise and Pantosti, 2001). During the Early-Middle Pleistocene, the end of shortening in the Southern Apennines occurred together with a major regional change in the stress regime from compressional-extensional to merely extensional. This work aims at providing information about the present-day tectonics of this area that reflects a new deformation stage in the regional geodynamics (Hippolyte *et al.*, 1994, 1995).

3. Crustal structure and seismicity

Information on the crustal structure of the Apennines mainly comes from gravity data (Giese and Morelli, 1975; Baldi *et al.*, 1982), deep seismic profiles (Cassinis *et al.*, 1979; Nicolich, 1989; Roeder, 1984) and seismic tomography (Chiarabba and Amato, 1997; Lucente *et al.*, 1999). All these geophysical observations reveal a variable Moho geometry (Geiss, 1987). Beneath the Tyrrhenian Sea the crust is 12 km thin and the Moho depth increase toward the Adriatic foreland, where geophysical investigations suggest depth at 38 km. The *P* wave tomographic images below the Apenninic belt (Chia-

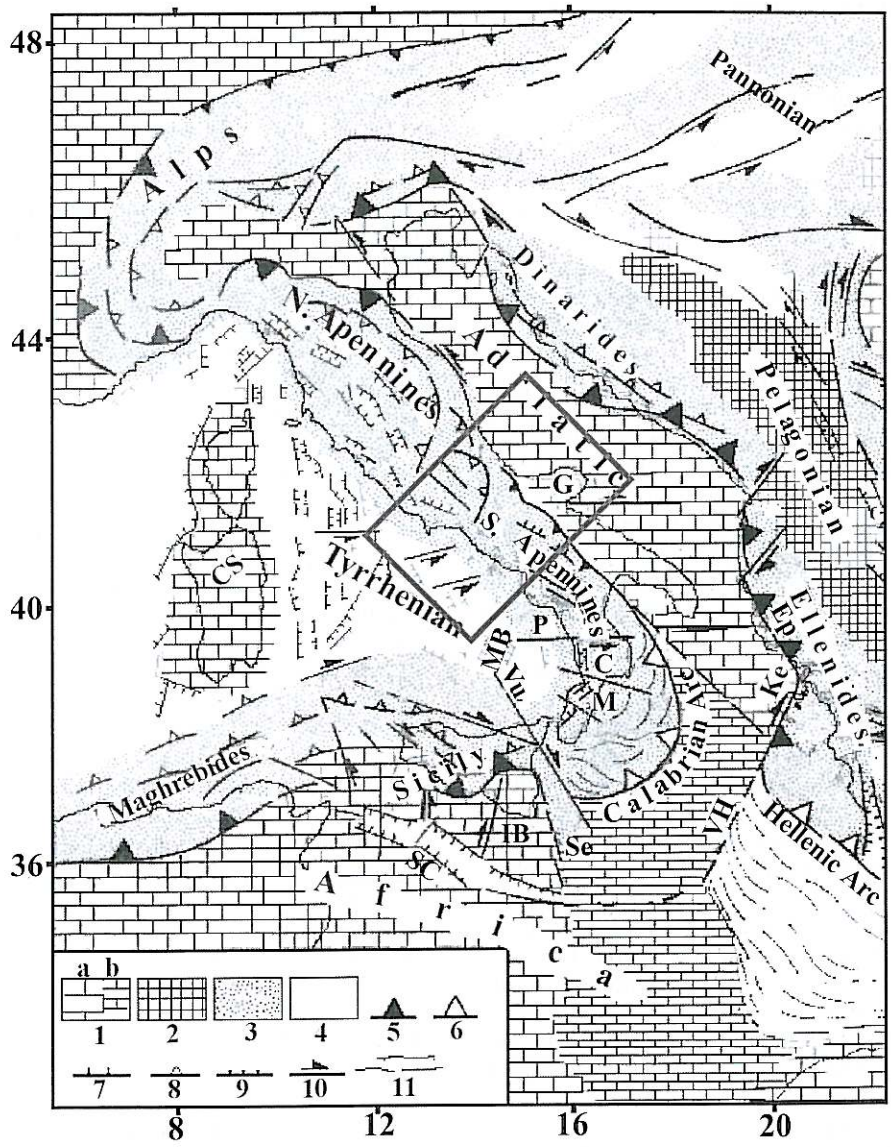

Fig. 1. The Central Mediterranean area: sketch of the major tectonic lineaments and structural domains (after Anzidei *et al.*, 2001; Mantovani *et al.*, 2000b). 1) Continental (a) and oceanic (b) parts of the Africa/Adriatic and Eurasian forelands; 2) Tethyan belt constituted by oceanic remnants and intermediate massifs; 3) deformation belts developed on the African and Eurasian margins; 4) crustal thinning; 5) active thrust fronts; 6) subduction zones; 7) inactive thrust fronts; 8,9,10) compressional, tensional and trascurrent features; 11) main trends of compressional deformations in the Mediterranean ridge and Calabrian arc. C = Crati trough; CS = Corsica-Sardinia block; Ep = Epirus; G = Gargano fault; Ke = Kefallinia fault; IB = Iblean block; M = Messina trought; MB = Marsili basin; P = Palinuro fault; SC = Sicily Channel; Se = Siracusa escarpment; Vu = Vulcano fault. The dark gray rectangle represents the sector of the GeoModAp-GPS network object of this study.

rabba and Amato, 1997; Lucente *et al.*, 1999) provide information on the structure and thermal regime of the deep crust. Generally, there is a good agreement between tomographic images and surface geological frame (Patacca and Scandone, 1989). A low velocity zone is present beneath the Latium-Abrutii limestone platform, ringed by high velocities, suggesting the presence of a different crust type. The Northern and Central-Southern Apennines are separated by a N-S trending lithological transition zone, the Ancona-Anzio lineament (Castellarin *et al.*, 1982), which separates the tectonic units of Umbria-Marche from the Latium-Abrutii platform. The agreement with tomography suggests that this discontinuity should be considered as a lateral structural boundary of the subducting Adriatic lithosphere (Lucente *et al.*, 1999). The tomographic images support the hypothesis that the region corresponding to the present Central-Southern Apennines was a continental promontory extending westward of the Adriatic plate (Lucente *et al.*, 1999). The Apulian carbonatic platform is evidenced beneath the Central-Southern Apennines at depth of ~ 10 km by deep seismic profiles and boreholes (Mostardini and Merlini, 1986; Amato and Montone, 1997). A continuous low velocity anomaly is present in the lower crust underneath the Northern and Southern Apennines arcs margin (Chiarabba and Amato, 1997) separated by a second low velocity anomaly along the Ortona-Roccamonfina lineament (Patacca *et al.*, 1990). Positive velocity anomalies are present beneath the Tyrrhenian side of the Apennines from the Alban hills (Latium) to the south (Flegrei fields). A low velocity belt is found all along the Tyrrhenian coast, in good agreement with the observed high heat flow, the thinning of the crust (Geiss, 1987), and the presence of quaternary volcanoes in the peri-Tyrrhenian area (Serri *et al.*, 1993).

The present seismicity distribution in the Italian Peninsula and Sicily (fig. 2) reflects the Neogene and Quaternary evolution of the Central Mediterranean. Seismic activity in the Italian Peninsula is mainly distributed along three longitudinal areas. The first is located along the Tyrrhenian side, with shallow (0-7 km depth) and small magnitude ($M < 4.5$) earthquakes, mostly concentrated in the vicinity of the Quaternary volcanoes and the geothermal areas, such as Tuscany, Latium and Campania. The second, belonging to the Apenninic belt, is generally characterized by stronger (M up to 7) and deeper (0-20 km depth) earthquakes, generally with normal (secondary strike-slip) focal mechanisms. The last concerns the Adriatic foredeep where seismic events also display thrust and strike-slip fault plane solutions in the Northern Apennines and in the Gargano area. The Tyrrhenian side is characterized by high thermal gradient and presence of magmatic/hydrothermal systems in the upper crust, which often generates episodes of vertical deformations (Flegrei fields, Albani hills). The Apenninic belt shows two distinct seismic regions, which differ for the total seismic moment, released, the largest magnitude observed and the faulting mechanism (Gasparini *et al.*, 1985; Frepoli *et al.*, 1996; Selvaggi *et al.*, 1997; Frepoli and Amato, 2000). The diffuse seismicity distribution within the area separating these two seismic districts (Cocco *et al.*, 1993) does not depict this region as a single fault zone, but rather as a transition zone (Ancona-Anzio lineament) between the Northern Apennines arc of Umbria and the carbonate platform of the Central Apennines. The Central and Southern Apennines are subjected to a sparse seismicity, less frequent than in Northern Apennines, but with larger magnitudes and strong historical earthquakes. Seismicity distribution in Central-Southern Apennines shows that the large tectonic discontinuities which played a fundamental role during the Apenninic built-up, like the Ancona-Anzio and the Ortona-Roccamonfina lineaments (Castellarin *et al.*, 1982; Patacca *et al.*, 1990), are no longer active, or that at least the deformation along these structures could be aseismic. Another interesting feature of the boundary region between Northern and Central-Southern Apenninic arcs is the different stress distribution. North of latitude 43°N, breakout data and focal mechanisms (Frepoli *et al.*, 1996; Montone *et al.*, 1997; Frepoli and Amato, 2000) reveal horizontal compression perpendicular to the thrust front in the external sector of the arc. At this latitude, a stress rotation is observed both at the external front and within the belt (Montone *et al.*, 1997), where NW-SE extension is suggested by fault-plane

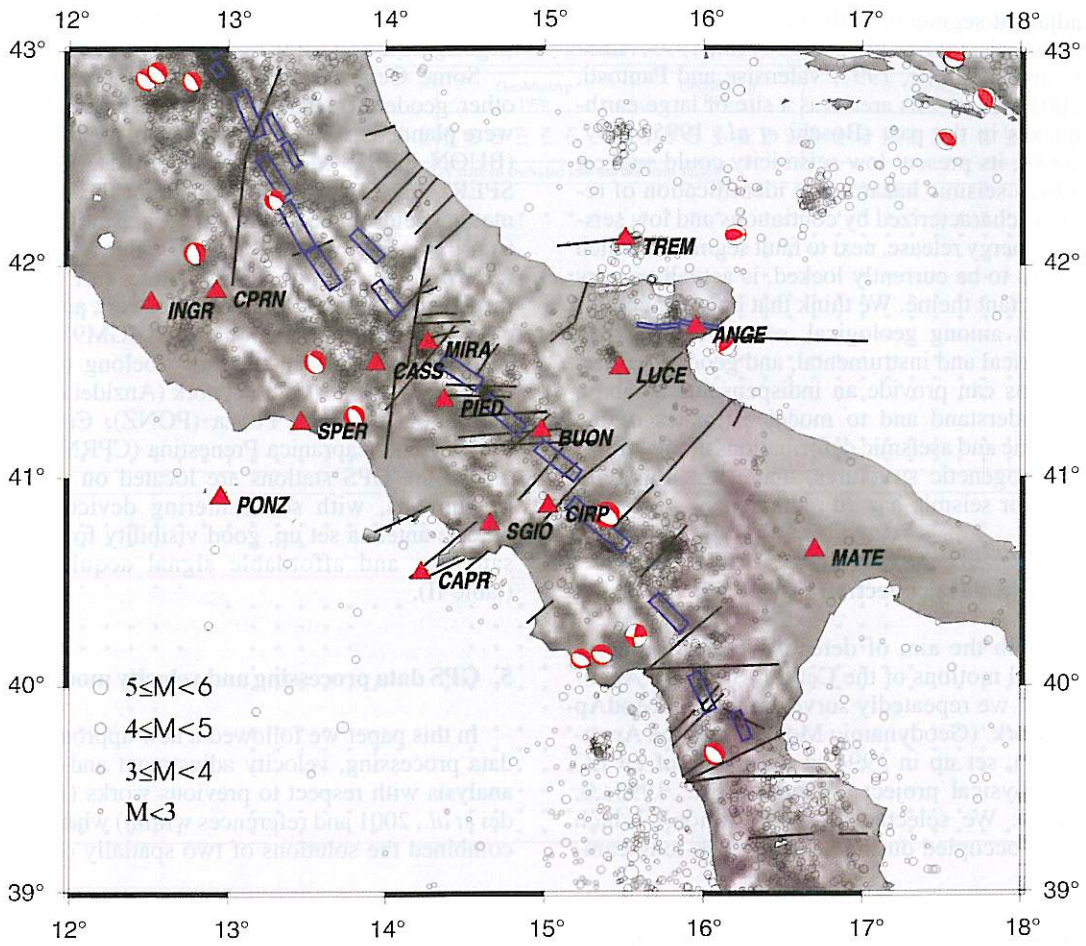

Fig. 2. Distribution of the GeoModAp GPS stations (red triangles) with respect to seismogenetic structures inferred from geological and geophysical data (blue boxes represent major fault segments and dark gray lines represent transverse and generic tectonic lineaments as provided by the Database of Potential Sources for Earthquakes Larger than M 5.5 in Italy, Release 1.0, Valensise and Pantosti, 2000), spatial distribution of instrumental seismicity from the INGV's bulletin for the time span 1985-1998 (gray circles, proportional to magnitude) and focal mechanisms for earthquakes with $M > 4.0$ from the Harvard CMT catalog.

solutions of recent crustal earthquakes (Frepoli *et al.*, 1996; Frepoli and Amato, 2000). During the last ten years new geophysical and geological studies (Valensise *et al.*, 1993; Boschi *et al.*, 1998; Gasperini *et al.*, 1999; Valensise and Pantosti, 2001) provide a fundamental tool for a better localization and identification of seismogenetic structures. Figure 2 shows part of the Database of Potential Sources for Earthquakes Larger than M 5.5 in Italy (Valensise and Pantosti, 2000). The Central-Southern Apennines are characterized by a narrow seismic belt, NW-SE striking and 30 to 50 km wide (Amato and Montone, 1997). In this area the seismicity is spatially clustered along the major fault segments (fig. 2) identifying the boundary between

adjacent segments of the main Southern Apennines seismic belt (Valensise *et al.*, 1993; Amato and Montone, 1997; Valensise and Pantosti, 2001). Since this area was a site of large earthquakes in the past (Boschi *et al.*, 1995, 1997, 2000), its present low seismicity could suggest a high seismic hazard. The identification of regions characterized by continuous and low seismic energy release, next to fault segments, which seems to be currently locked, is actually a very important theme. We think that only the combination among geological, seismological, both historical and instrumental, and geodetic observations can provide an indispensable database to understand and to model estimates of the seismic and aseismic deformations along known seismogenetic structures, that is an important tool for seismic hazard reduction.

4. GPS data collection

With the aim of detecting the present day crustal motions of the Central-Southern Apennines, we repeatedly surveyed the GeoModAp network (Geodynamic Modeling of the Apennines), set up in 1994 in the frame of an EC geophysical project (Anzidei *et al.*, 1995a,b, 2001). We selected 15 GPS stations, which were occupied during several week-long campaigns in 1994, 1995, 1996, 1999 and 2000 (fig. 2, table I).

Some GeoModAp GPS stations belong to other geodetic networks, and seven new sites were planned and established during the project (BUON, CIRP, MIRA, INGR, PIED, SGIO, SPER), in order to better constraint the deformation field of the chain. The four stations of Capri (CAPR), Lucera (LUCE), Sant'Angelo (ANGE) and Tremiti (TREM), are part of to the first order Italian Geodetic Network and are coincident with the National GPS IGM95 network (Surace, 1997); they also belong to the regional Tyrgeonet GPS network (Anzidei *et al.*, 2001) together with Ponza (PONZ), Cassino (CASS) and Capranica Prenestina (CPRN).

All the GPS stations are located on stable monuments, with self-centering devices for precise antenna set up, good visibility for GPS satellites and affordable signal acquisition (table II).

5. GPS data processing and velocity modeling

In this paper we followed a new approach in data processing, velocity adjustment and error analysis with respect to previous works (Anzidei *et al.*, 2001 and references within) where we combined the solutions of two spatially differ-

Table I. Complete names and labels used for the GeoModAp GPS stations. Connection with other Italian geodetic networks. Type of monumentation (1 - concrete pillar; 2 - marker screwed in stable outcrops; 3 - stable building; 4 - concrete pillar built on the roof of a stable building). The last five columns describe the receiver-antenna combination for each survey.

GeoModAp GPS network					1994	1995	1996	1999	2000
Complete name	Label	Institutions	Connected network	Type	Receiver-antenna	Receiver-antenna	Receiver-antenna	Receiver-antenna	Receiver-antenna
Mnt. San'Angelo	ANGE	IGM	IGM 1th ord. - IGM95	4	ASHL12-ASH700228A	TRMSST-TRM14532.00	ASHZ12-ASH700228D	TRMSSI-TRM22020.00	TRMSSI-TRM22020.00
Buonalbergo	BUON	INGV		2	TRMSSE-TRM22020.00	ASHM12-ASH700228D	TRMSSI-TRM22020.00	TRMSSI-TRM22020.00	TRMSSI-TRM22020.00
Capranica Prenestina	CPRN	INGV	Colli Albani, Rome	2		TRMSSE-TRM22020.00	ASHM12-ASH700228D	ASHZ12-ASH700228D	TRMSSI-TRM22020.00
Capri	CAPR	IGM	IGM 1th ord. - IGM95	3	SR299-LEISR299_INT	SR299- LEISR299_INT	SR299- LEISR299_INT	TRMSSI-TRM22020.00	TRMSSI-TRM22020.00
Cassano Irpino	CIRP	INGV	Napoli	1	TRMSSE-TRM22020.00	TRMSSE-TRM14532.00	TRMSSI-TRM22020.00	TRMSSI-TRM22020.00	TRMSSI-TRM22020.00
Cassino	CASS	ENEA - IGM	Cassino - IGM95	1	ASHL12-ASH700228A	ASHM12-ASH700228D	ASHZ12-ASH700228D	TRMSSI-TRM22020.00	TRMSSI-TRM22020.00
INGV	INGR	INGV	Napoli	4		TRMSSE-TRM22020.00	TRMSSE-TRM22020.00	TRMSSI-TRM22020.00	TRMSSI-TRM22020.00
Lucera	LUCE	IGM	IGM 1th ord. - IGM95	1	ASHL12-ASH700228A		ASHZ12-ASH700228D	TRMSSI-TRM22020.00	
Miranda	MIRA	INGV		2	TRMSSE-TRM22020.00	TRMSSE-TRM22020.00	TRMSSE-TRM22020.00	TRMSSI-TRM22020.00	TRMSSI-TRM22020.00
Piedimonte Matese	PIED	INGV		2		TRMSSE-TRM22020.00	TRMSSE-TRM22020.00	TRMSSI-TRM22020.00	TRMSSI-TRM22020.00
Ponza	PONZ	IGM-INGV	Italian Magnetic Netw.	1	TRMSST-TRM14532.00	TRMSSE-TRM22020.00	TRMSSE-TRM22020.00	TRMSSI-TRM22020.00	TRMSSI-TRM22020.00
San Giorgio	SGIO	Oss.Vesuviano	Napoli	2		TRMSSE-TRM14532.00	TRMSSE-TRM14532.00	TRMSSE-TRM22020.00	TRMSSI-TRM29659.00
Sperlonga	SPER	INGV		2		TRMSSE-TRM22020.00	TRMSSE-TRM22020.00	TRMSSI-TRM22020.00	TRMSSI-TRM22020.00
Tremiti	TREM	IGM	IGM 1th ord. - IGM95	4	TRMSST-TRM14532.00	ASHM12-ASH700228D	TRMSSI-TRM22020.00	TRMSSI-TRM22020.00	TRMSSI-TRM22020.00

Table II. Daily occupation table for the GeoModAp network and the IGS and other GPS permanent stations included into the analysis of the primary regional observations.

Survey	GeoModAp 1994					GeoModAp 1995										GeoModAp 1996							GeoModAp 1999						GeoModAp 2000										
Session	320	321	322	323	324	168	169	170	171	172	173	174	175	176	177	170	171	172	173	174	175	176	177	137	138	139	140	141	142	143	159	160	161	162	163	164	165	166	167	168	169	170
Permanent IGS stations included into the first step analysis																																									
AQUI																															•	•	•	•	•	•	•	•	•	•	•
CAGL																•	•	•	•	•	•	•	•	•	•	•	•	•	•	•	•	•	•	•	•	•	•	•	•	•	•
CAME																															•	•	•	•	•	•	•	•	•	•	•
COSE																								•	•	•	•	•	•	•	•	•			•	•	•				
GRAZ	•	•	•	•	•			•	•	•	•	•	•	•	•	•	•	•	•	•	•	•	•	•	•	•	•	•	•	•	•	•	•	•	•	•	•	•	•	•	•
LAMP																								•	•	•	•	•	•	•	•	•	•	•	•	•	•	•	•	•	•
MATE	•	•	•	•	•	•	•	•	•	•	•	•	•	•	•	•	•	•	•	•	•	•	•	•	•	•	•	•	•	•	•	•	•	•	•	•	•	•	•	•	•
NOTO																•	•	•	•	•	•	•	•	•	•	•	•	•	•	•	•	•	•	•	•	•	•	•	•	•	•
UNPG																								•	•	•	•	•	•	•	•	•	•		•	•	•	•	•	•	•
UPAD										•		•	•	•	•	•	•	•	•	•	•	•	•		•	•	•	•	•	•	•	•	•	•	•	•	•	•	•	•	•
VVLO																															•	•	•		•	•	•	•	•	•	
WETT	•	•	•	•	•	•	•	•	•	•	•	•	•	•	•	•	•	•	•	•	•	•	•																		
WTZR																•	•	•	•	•	•	•	•	•	•	•	•	•	•	•	•	•	•	•	•	•	•	•	•	•	•
ZIMM	•	•	•	•	•	•	•	•	•	•	•	•	•	•	•	•	•	•	•	•	•	•	•	•	•	•	•	•	•	•	•	•	•	•	•	•	•	•	•	•	•
GeoModAp GPS stations																																									
ANGE	•	•	•	•	•	•	•	•	•	•	•	•	•	•	•	•	•	•	•	•	•	•	•	•	•	•	•	•	•	•	•	•	•	•	•	•	•				
BUON	•	•	•	•	•			•	•	•										•	•	•			•	•	•								•	•	•	•			
CAGI	•	•	•	•																																					
CAPI	•	•		•	•																																				
CAPR							•	•	•	•	•	•	•	•	•		•	•	•	•	•	•			•	•	•	•	•	•			•	•	•	•	•	•	•	•	•
CASS	•	•	•	•				•	•	•	•	•	•				•	•	•						•	•	•	•			•	•	•							
CIRP	•	•	•	•	•			•	•	•	•	•	•				•	•	•					•	•	•	•	•	•		•	•	•	•	•	•	•	•	•	
CPRN								•	•								•	•	•	•	•	•									•	•	•	•	•					
INGR								•	•	•	•	•	•			•	•	•	•	•				•	•	•	•	•	•	•	•	•	•	•	•	•	•	•	•	•	
LUCE			•	•																•	•	•						•	•	•										
MIRA	•	•						•	•	•	•	•	•				•	•	•		•	•						•	•	•					•	•	•	•	•	•	
PIED								•	•	•	•	•	•	•	•		•	•	•	•	•			•	•	•	•	•	•	•	•	•	•	•	•	•				
PONZ	•	•	•	•	•			•	•	•	•	•	•				•	•	•	•	•				•	•	•	•	•	•		•	•	•	•	•	•	•	•	•
SGIO									•	•	•	•	•				•	•	•	•		•			•	•	•	•						•	•	•				
SPER								•	•	•	•	•	•			•	•	•	•	•	•	•	•	•	•	•	•	•	•				•	•	•	•	•				
TREM	•	•	•	•	•			•	•	•		•	•				•	•	•	•		•			•	•	•				•	•	•	•	•	•	•	•	•	•

ent networks obtained with different processing schemes and software versions. The obtained differences are not statistically significant even in terms of velocity field and strain rate field, except for errors, which are lower in this last computation due to the extremely self-consistency of the GeoModAp network and of the data processing approach (Dong *et al.*, 1998).

We processed and analyzed GPS data following three main computing steps, using the GAMIT/GLOBK (King and Bock, 1995; Herring, 1999) and QOCA software (Dong *et al.*, 1998; http://gipsy.jpl.nasa.gov/qoca).

In the first step we used GAMIT to analyze the GPS carrier phase data for the regional GPS network, including some IGS European stations (at least MATE, NOTO, CAGL, WTZR, ZIMM, GRAZ) to frame the regional network to the ITRF coordinate system.

We adopted the IGS_1 model in the data processing, in order to take into account the antenna phase center variations as a function of the elevation of satellites (Rothacher and Mader, 1996). This model arbitrarily assumes no elevation-dependent terms for Dorne-Margolin choke ring antennas and applies elevation-dependent variations for other antennas.

Satellite *a priori* orbits are obtained by numerically integrating the initial conditions (g-files) obtained from SOPAC (Script Orbit and Permanent Array Center) products archive. Using these satellites ephemerides, along with *a priori* values for station coordinates, Earth rotation parameters and standard expressions for the precession and nutation, GAMIT computes theoretical values for the carrier phase observations at both the L1 and L2 frequencies for each station-satellite combination. These values are

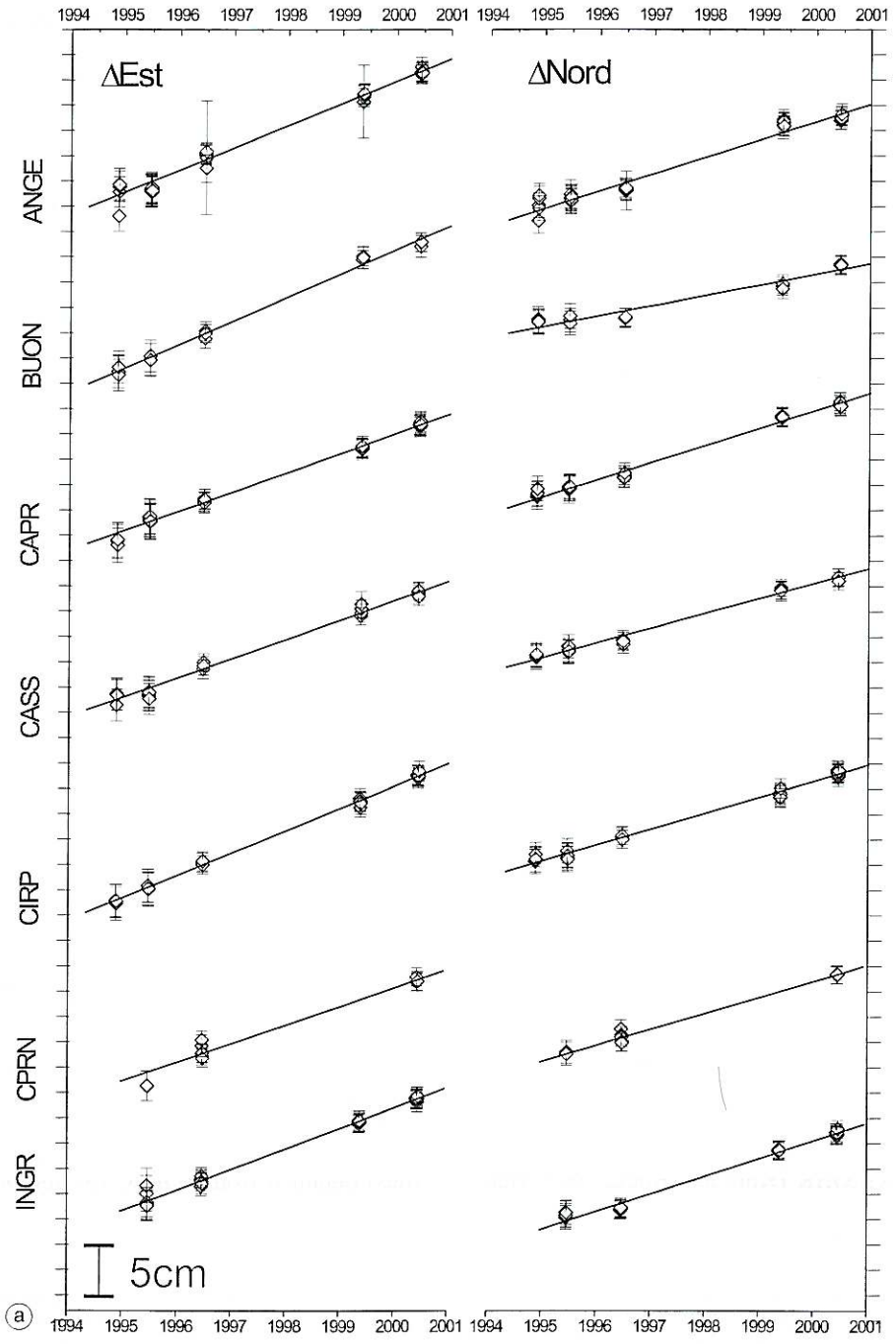

Fig. 3a,b. Time series for the GeoModAp-GPS stations. Coordinates are obtained in the separate mode QOCA analysis, constraining at the centimeter level some IGS permanent stations to their ITRF97 values.

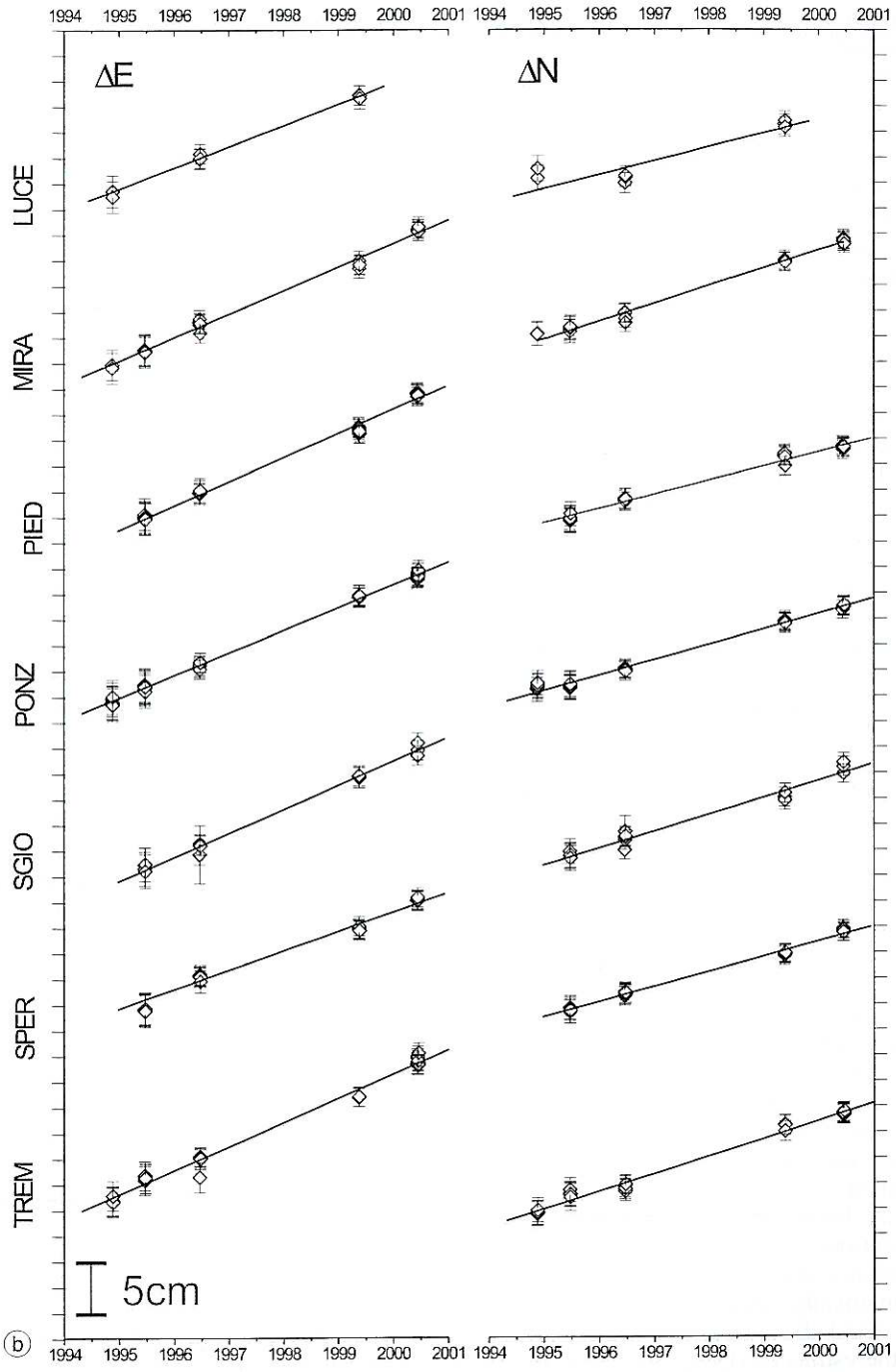

Fig. 3a,b (*continued*).

then subtracted from the observed ones to form phase residuals and combined as double differences (between satellites and between sites) in a least square analysis to estimate station coordinates, orbital and phase ambiguity parameters (Shaffrin and Bock, 1988). Residual tropospheric effects respects to a reference model (*e.g.*, Saastamoinen, 1972) are parameterized by a combination of zenith delay parameters. The product of the single-session analysis is a set of loosely constrained parameters estimates and their covariance matrix. The first step of the process is the ambiguity resolution, that is the evaluation of their correct integer numbers, in order to eliminate them from the observation equations. This is performed through a series of four intermediate solutions, executed sequentially in a series of scripts of the GAMIT automatic processing scheme: 1) All parameters are estimated using the ionospheric-free (LC) combination of the L1 and L2 phase, imposing thigh constraints on some station coordinates. 2) Holding the geodetic parameters fixed at the values obtained previously, the wide-lane (L5) ambiguity parameters are estimated and, if possible, constrained to integer values; ionospheric refraction is constrained by the introduction of a further observation equation in a «geometry-free» combination (Dong and Bock, 1989). If precise pseudoranges at both the L1 and L2 frequencies are available, they are used to help the determination of the wide-lane ambiguities. 3) The equations of «iono-free» combination are solved, fixing the wide-lane ambiguities, and resolving the residual biases of these observables (narrow lane). As in solution 1, a reference frame is defined by imposing tight constraints on some station coordinates. 4) Using the resolved values of both the wide-lane and narrow-lane ambiguities held fixed, the final values of geodetic parameters are estimated from LC observations. In order to produce the loose constrained parameters estimates, solutions 1 and 4 are repeated with orbit and position constraints sufficiently tight to avoid numerically singularity, but sufficiently loose to avoid the introduction of significant bias on the estimates (Dong and Bock, 1989; Dong *et al.*, 1998). Using this processing scheme, loose constrained solutions for each session of the surveys from 1994 to 2000 were obtained.

In the second step, we combined all the daily regional loose constrained solutions with the global loose constrained solutions provided by SOPAC (h-files) for the same period, solving the commonly shared parameters, such as the satellites orbits and the coordinates of the global IGS permanent stations included in both the subsets, by means of the Kalman filter procedure included in the GLOBK software. Oral (1994) and Zhang (1996) have demonstrated that the combination of global and regional solutions through an adjustment of their corresponding estimates, and using full covariance matrices, yields parameter estimates that are statistically equivalent to a simultaneous adjustment using all the data; this approach is significantly more efficient and maintains reasonable homogeneous solutions.

The third step was performed by combining all regional and global loose constrained daily solutions as quasi observation to model the velocity of each station, assumed to be constant in time, by means of the QOCA software. The combination was performed through the sequential Kalman filtering, allowing global translation and rotation for each daily solution. Random walk style perturbations were allowed for some parameters whose errors were correlated with time, such as the Earth Orientations Parameters and the antenna heights (Rothacher *et al.*, 1996; Dong *et al.*, 1998). We first analyzed the time series in order to detect outliers which may be due to missing antenna height record, wrongly fixed cycle slip, severe multipath, poor satellite configuration and other blunders not evidenced during the previous data analysis. As a rule of thumb we adopted the self-consistency, so, if one quasi observation is significantly inconsistent with the other, this data is likely to be an outlier. Figures 3a and 3b show the time series for the 14 stations of the GeoModAp network, and confirms that the assumption of a constant velocity is reasonable. The reference frame is defined only in this last step, and it affords for a rigorous solution to the problem of an inhomogeneous tracking network, where the set of stations changes from day to day and year to year (Feigl *et al.*, 1993). Since the fidu-

Table III. Constraint and perturbations used in the global analysis with QOCA (for more details please see Dong *et al.*, 1998).

GPS analysis constraints	Horizontal (m)	Vertical (m)	Perturbation m^2/yr
IGS coordinates	0.1	0.5	0.004 (V)
IGS velocities	Fixed	0.01	0.004 (V)
GeoModAp coordinates	10	10	0.004 (V)
GeoModAp velocities	1.0	1.0	0.004 (V)
Equatorial rotation	30 mas		730 mas^2/yr
Axial rotation	0.5 mas		0.5 mas^2/yr
Translation	1 m		300 mas^2/yr

cial network define the frame to which the estimated vectors are referred, simply comparing a vector estimated on two days with different networks can lead to an inaccurate estimate of its rate of change. The approach adopted in this work minimizes the effect of the shifting fiducial geometry by imposing the constraints on the coordinates and on the velocities in a consistent manner. This is particularly important for GPS tracking stations that have been used only few times (as WETT and CAGL). We obtained the velocity field in the ITRF97 reference frame tightly constraining the velocities of some European IGS permanent stations listed in table II. The constraints applied and the perturbations used are listed in table III.

To assess the accuracy of the velocity field obtained in this last step we took into account the complexity of the error spectra of GPS data. A spatial correlation may be due to the common orbital, Earth rotation, and regional atmospheric errors (Feigl *et al.*, 1993), while a temporal correlation is induced by atmospheric disturbance, monument instability and orbital misfits (Zhang *et al.*, 1997; Mao *et al.*, 1999).

Following the error analysis proposed by Dong *et al.* (1998), we used the empirical approach described in Shen *et al.* (2000). At each step, when a new data file was added, we considered the increment of the postfit χ^2 due to the addition of the new data file and the increase of degrees of freedom in data space, evaluated in a conventional way (observation number estimated parameter number). Each data file was then re-weighted after the iteration using the square root of the $\delta\chi^2$ per quasi observation data file averaged from forward and backward Kalman filtering (see tables IV and V). This procedure allows an adequate relative weighting for the individual data files. The next step was to evaluate the increase of the number of parameters caused by allowing the parameters perturbation in the Kalman filtering process. The total normalized RMS has been then be revaluated with an updated estimate of the number of degrees of freedom and then the velocity error – has been rescaled.

Sometimes a high value of $\delta\chi^2$ per quasi observation should not come from the underestimated formal uncertainty, but another possibility is that two adjacent quasi observation files have close observation epochs but with completely different rotational status (Dong *et al.*, 1998). In this case, the assigned global network parameter perturbation level is not adequate to account for the different network rotation, so we enlarged the perturbation level for this quasi observation file.

In order to give the residual velocity field with respect to an Eurasian fixed reference frame (table VI), we rotate our ITRF97 velocity solutions using the rotation pole given by the NUVEL-1A model (DeMets *et al.*, 1994). Since we are mainly interested in the relative movements between GeoModAp stations for the estimation of the present-day strain rate of the Apennines, the definition of a fixed Eurasian reference frame is out of the scope of this work. Figure 4 shows the residual velocities of GeoModAp stations (red arrows) after the rotation into the «Eurasian fixed» reference frame.

Table IV. Reference epoch, initial weighting factor, number of observation, $\delta\chi^2$ per quasi observation, both for forward and backward filtering and final reweighting factor per quasi observation data file.

QOB num.	Julian day	QOB epoch	Initial rew. fact.	Observation number	$\delta\chi^2$ forward	$\delta\chi^2$ backward	Final rew. fact.
1	320	1994.8747	1.00	48	0.003	2.446	1.11
2	321	1994.8775	1.00	51	0.674	2.316	1.22
3	322	1994.8802	1.00	48	0.857	3.803	1.53
4	323	1994.8830	1.00	51	0.660	5.863	1.81
5	324	1994.8857	1.00	45	0.751	3.792	1.51
6	168	1995.4579	1.00	30	2.758	0.394	1.25
7	170	1995.4606	1.00	33	1.473	0.612	1.00
8	171	1995.4634	1.00	66	0.813	1.071	1.00
9	172	1995.4661	1.00	69	1.166	2.135	1.28
10	173	1995.4689	1.00	69	0.855	1.840	1.16
11	174	1995.4716	1.00	60	0.669	2.231	1.20
12	175	1995.4743	1.00	66	0.788	2.570	1.29
13	176	1995.4771	1.00	45	0.545	2.521	1.24
14	177	1995.4798	1.00	42	0.453	3.101	1.33
15	170	1996.4627	1.00	42	2.626	0.555	1.26
16	171	1996.4654	1.00	69	2.799	0.956	1.37
17	172	1996.4682	1.00	66	2.794	1.953	1.54
18	173	1996.4709	1.00	69	1.701	2.696	1.48
19	174	1996.4736	1.00	66	0.503	1.351	1.00
20	175	1996.4764	1.00	63	0.547	2.485	1.23
21	176	1996.4791	1.00	63	0.734	5.701	1.79
22	177	1996.4819	1.00	39	0.671	3.029	1.36
23	137	1999.3730	1.00	42	6.297	0.480	1.84
24	138	1999.3758	1.00	60	5.383	0.621	1.73
25	139	1999.3785	1.00	60	1.220	0.600	1.00
26	140	1999.3812	1.00	63	1.482	0.806	1.09
27	141	1999.3840	1.00	63	2.115	1.251	1.29
28	142	1999.3867	1.00	54	0.811	0.480	1.00
29	143	1999.3895	1.00	48	0.533	0.811	1.00
30	159	2000.4326	1.00	60	3.174	0.242	1.31
31	160	2000.4353	1.00	63	2.022	0.285	1.07
32	161	2000.4381	1.00	69	2.250	0.377	1.15
33	162	2000.4408	1.00	69	1.301	0.330	1.00
34	163	2000.4435	1.00	69	1.375	0.383	1.00
35	164	2000.4463	1.00	72	2.201	0.415	1.14
36	165	2000.4490	1.00	72	1.917	0.178	1.02
37	166	2000.4517	1.00	66	0.810	0.193	1.00
38	167	2000.4545	1.00	54	0.500	0.257	1.00
39	168	2000.4752	1.00	54	0.615	0.257	1.00
40	169	2000.4600	1.00	54	0.651	0.127	1.00
41	170	2000.4627	1.00	42	0.441	0.001	1.00

Table V. Statistic of the final QOCA global solution (OBS = total observation number; SITES = total number of sites from data files; PARA = total estimate parameters; CONST = constraints reduced parameters dimension; PERTU = perturbation increased parameters dimension; DOF = degrees of freedom; NRMS = normalized rms); for more details refer to Dong *et al.* (1998).

QOB files	OBS	SITES	PARA	CONST	PERTU	DOF	NRMS
41	2334	26	163	26.5379	649.706177	1547.832	1.22004254

Table VI. Final velocity solution and errors. Velocities are given both in the ITRF97 reference frame and with respect to an Eurasian Fixed reference frame (NUVEL-1A, DeMets *et al.*, 1994).

Site	Long.	Lat.	Velocity mm/yr ITRF97		Uncertainty mm/yr		Correlation coefficient	Residual Velocity mm/yr	
			East	North	East	North		East	North
IGS permanent stations									
CAGL	8.973	39.136	20.9	13.1	0.1	0.1	0.002	0.19	−0.79
GRAZ	15.494	47.067	21.8	13.5	0.1	0.1	−0.003	1.06	−0.79
HERS	0.336	50.867	17.2	15.0	0.1	0.1	−0.005	−0.16	0.03
KOSG	5.810	52.178	17.0	14.4	0.1	0.1	−0.006	−1.24	0.14
MAS1	344.367	27.764	16.8	15.3	0.1	0.1	0.001	−1.60	−0.82
MATE	16.705	40.649	23.5	17.4	0.1	0.1	0.002	1.79	4.79
NOTO	14.990	36.876	21.9	17.5	0.1	0.1	−0.002	0.17	4.59
ONSA	11.926	57.395	17.1	13.3	0.1	0.1	−0.010	−1.28	−0.09
UPAD	11.878	45.407	21.6	15.7	0.1	0.1	−0.002	1.23	2.33
VILL	356.048	40.444	18.3	14.0	0.1	0.1	−0.001	−0.11	−1.37
WTZR	12.879	49.144	20.1	13.5	0.1	0.1	−0.018	0.11	0.22
ZIMM	7.465	46.877	19.2	14.0	0.1	0.1	−0.013	−0.24	−0.06
GeoModAp Stations									
ANGE	15.952	41.708	23.1	16.6	0.2	0.2	−0.004	1.63	3.86
BUON	14.982	41.221	23.3	10.4	0.3	0.3	0.001	1.90	−2.46
CAPR	14.224	40.545	19.0	16.7	0.2	0.2	0.000	−2.31	3.63
CASS	13.937	41.542	19.6	14.2	0.3	0.3	0.009	−1.56	1.12
CIRP	15.024	40.862	21.8	15.8	0.2	0.2	−0.009	0.38	2.93
CPRN	12.928	41.881	20.2	15.4	0.3	0.3	0.030	−0.74	2.16
INGR	12.515	41.828	20.6	16.6	0.2	0.2	−0.006	−0.29	3.25
LUCE	15.473	41.517	20.6	14.6	0.8	0.9	−0.018	−0.83	1.74
MIRA	14.266	41.640	22.7	16.5	0.2	0.2	0.011	1.44	3.52
PIED	14.369	41.366	23.1	13.7	0.2	0.2	−0.006	1.87	0.74
PONZ	12.953	40.908	21.6	14.9	0.2	0.2	−0.001	0.54	1.66
SGIO	14.657	40.777	22.6	15.9	0.3	0.4	0.080	1.23	2.99
SPER	13.464	41.259	20.2	14.3	0.2	0.2	0.007	−0.89	1.13
TREM	15.507	42.122	22.9	16.8	0.2	0.2	−0.001	1.58	3.98

6. Strain rate computation

The relatively high spatial density of the GeoModAp network, with respect to the other regional GPS networks presently surveyed in the Italian area (Vespe *et al.*, 2000; Anzidei *et al.*, 2001), allows us to estimate the strain rate for the study area. We used the GPS velocities weighted by their uncertainties to estimate the two-dimensional velocity gradient tensor and related parameters, such as the strain rate tensor, maximum and minimum eigenvalues, dilatation and rotation rates (Feigl *et al.*, 1990, 1993). From the velocity field, the strain rate may be computed solving for the velocity gradient tensor L (Malvern, 1969) over a sub-network, defined by a group of stations, or over the whole network. The velocity gradient tensor can be defined as $L = \dot{E} + \dot{W}$. The symmetric part of L, $\dot{E}$, is the strain rate tensor. The anti-symmetric part of L, $\dot{W}$, gives a local measure of the vorticity, or rate of rotation. For the two-dimensional case, L can be written as

$$L = \begin{bmatrix} \dot{E}_{11} & \dot{E}_{12} \\ \dot{E}_{21} & \dot{E}_{22} \end{bmatrix} + \begin{bmatrix} 0 & \dot{w} \\ -\dot{w} & 0 \end{bmatrix}.$$

We used two different methods to obtain the planar velocity gradient tensor. The first one computes the strain rate tensor over the whole network, or within subnetworks (Feigl *et al.*,

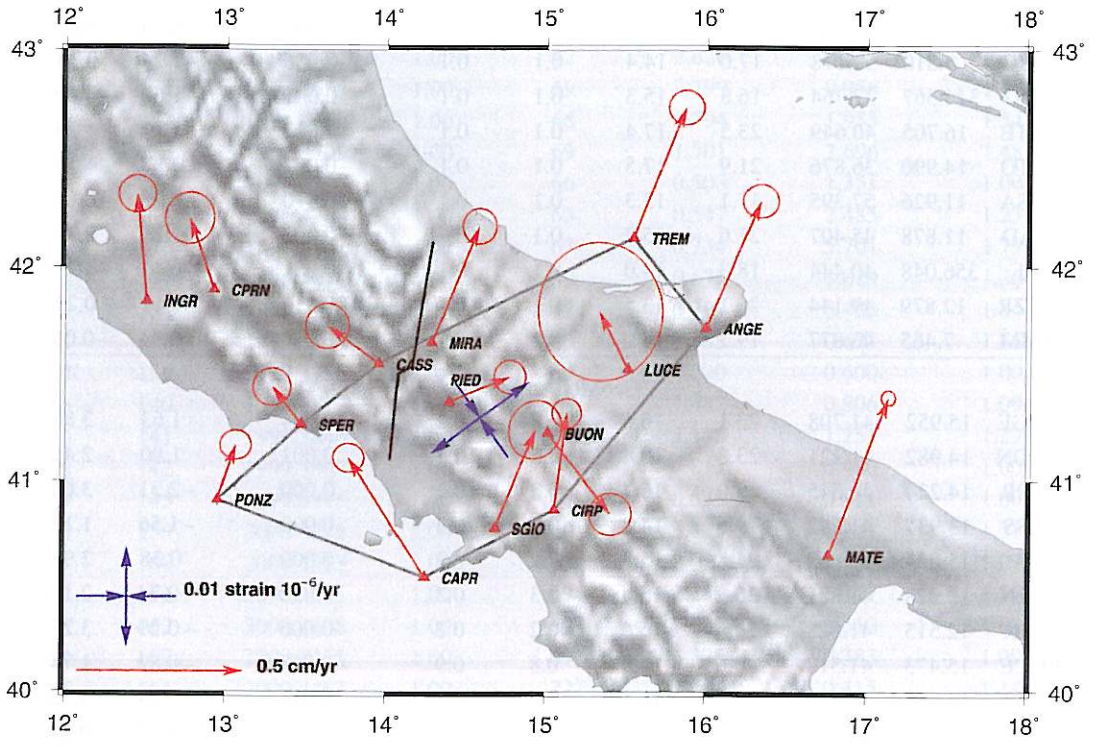

Fig. 4. GeoModAp residual velocity field with respect to a fixed Eurasian reference frame (NUVEL-1A model, De Mets *et al.*, 1994). Error ellipses are at the 95% confidence level. The dark gray line represents the position of the Ortona-Roccamonfina tectonic line, which separates the Northern Apennines arc from the Southern Apennines arc. The black line represents the polygon used for the computation of the averaged strain rate plane tensor (blue arrows). See table VII for numerical values and errors of strain rates.

Table VII. Strain rate values and errors computed within the whole network and subnetworks (refer to figs. 4 and 5 for subnetworks geometry) using the approach of Feigl *et al.* (1990).

Long. (deg)	Lat. (deg)	E_{max} (1/yr)	σE_{max} (1/yr)	E_{min} (1/yr)	σE_{min} (1/yr)	Cw-Spin (1/yr)	σ Spin (1/yr)	Theta (deg)	σ Theta (deg)	Network name
14.465	41.327	1.37E-08	6.92E-10	−4.74E-09	7.60E-10	9.07E-10	5.15E-10	−25.79	1.601	Full network
14.565	41.292	1.22E-08	7.84E-10	−9.87E-09	1.29E-09	4.16E-09	7.51E-10	−35.85	1.950	fig. 4
13.160	41.485	1.66E-08	2.07E-09	−2.23E-08	2.54E-09	2.21E-09	1.64E-09	62.52	2.403	Subnet. A - fig. 5
13.826	40.874	−6.37E-09	3.07E-09	−2.90E-08	3.26E-09	2.68E-09	2.18E-09	−21.76	5.497	Subnet. B - fig. 5
14.387	41.239	2.56E-08	2.50E-09	−1.16E-08	2.60E-09	1.23E-08	1.75E-09	−12.63	2.693	Subnet. C - fig. 5
15.199	41.513	1.45E-08	1.46E-09	−9.57E-10	1.99E-09	2.59E-09	1.27E-09	112.84	4.519	Subnet. D - fig. 5
15.894	41.075	1.56E-08	1.67E-09	−4.06E-09	1.62E-09	−3.65E-09	1.18E-09	−23.72	3.413	Subnet. E - fig. 5

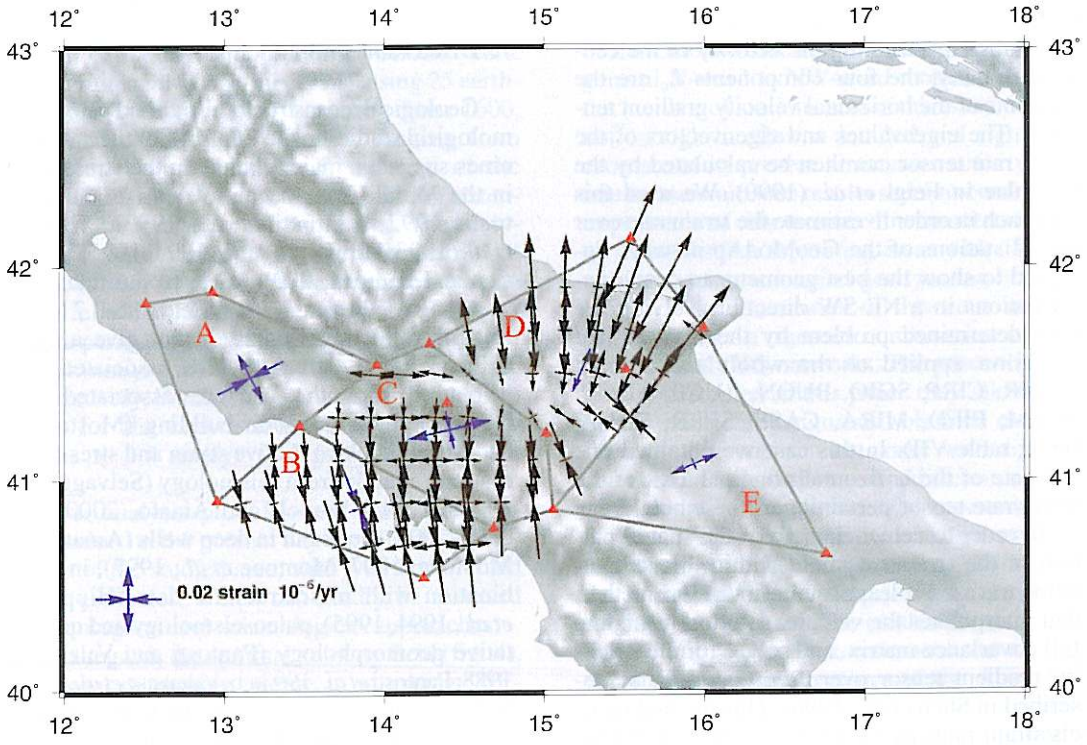

Fig. 5. Spatial pattern of strain rates (black arrows) computed using the approach of Shen *et al.* (1996), within the transect of the 12 stations used for the computation of the averaged strain rate tensor shown in fig. 4. We subdivided the area of the GeoModAp network into subnetworks that show a quite homogeneous strain rate field (dark gray lines), and for each of these subnetwork we computed the plane strain rate tensor solving the over determined least square problem (Feigl *et al.*, 1990, 1993). See table VII for numerical values of strain rates and errors.

1990, 1993). Given the velocities and their accuracies for at least three stations, we can estimate the horizontal velocity gradient tensor L by solving the inverse problem

$$\begin{bmatrix} 1 & 0 & \Delta x_1 & \Delta y_1 & 0 & 0 \\ 0 & 1 & 0 & 0 & \Delta x_1 & \Delta y_1 \\ 1 & 0 & \Delta x_2 & \Delta Y_2 & 0 & 0 \\ 0 & 1 & 0 & 0 & \Delta x_2 & \Delta Y_2 \\ \vdots & \vdots & \vdots & \vdots & \vdots & \vdots \\ 1 & 0 & \Delta y_N & \Delta y_N & 0 & 0 \\ 0 & 1 & 0 & 0 & \Delta x_n & \Delta y_n \end{bmatrix} \begin{bmatrix} u_0 \\ v_0 \\ L_{11} \\ L_{12} \\ L_{21} \\ L_{22} \end{bmatrix} = \begin{bmatrix} u_1 \\ v_1 \\ u_2 \\ v_2 \\ \vdots \\ u_n \\ v_n \end{bmatrix}$$

Where Δx_i and Δy_i is the east and north coordinates of the i-th station relative to the centroid of the network. The velocities u and v are in the east and north directions, respectively, with the zero subscript denoting the velocity of the centroid. Finally, the four components L_{ij} are the elements of the horizontal velocity gradient tensor L. The eigenvalues and eigenvectors of the strain rate tensor can then be calculated by the formulae in Feigl *et al.* (1990). We used this approach in order to estimate the strain rate over the 12 stations of the GeoModAp network designed to show the best geometry to detect deformations in a NE-SW direction, solving the over determined problem by the least square inversion applied to the whole subnetwork (CAPR, CIRP, SGIO, BUON, LUCE, ANGE, TREM, PIED, MIRA, CASS, SPER, PONZ; fig. 4; table VII). In this case we obtained one estimate of the horizontal principal axes of the strain rate tensor pertaining to the whole area.

In order to detect changes in the spatial pattern of the strain rate field within this subnetwork we used a least square inversion method that interpolates the velocity solution, using the full covariance matrix, and solves for the velocity gradient tensor over a regular grid, as described in Shen *et al.* (1996). This method models strain rates as a continuous function within the network. By this approach we obtained the velocity components, rotation rate and strain rate components at each node of a regular grid, whose dimension is defined by the spatial distribution of GPS stations (fig. 5). The algorithm uses a particular weighting scheme, with smoothing constant with distance, that acts as a filter for the selection of the number of GPS velocity vectors that will be included in the least square inversion, and that downweights the contribute of the velocities of stations at a certain distance (for more details see Shen *et al.*, 1996). Since we are interested in the mean strain rate trend along this sector of the Apennines, and we think that the number of available GPS stations does not allow a significant local analysis, we used as smoothing constant a value of 100 km, which is the baseline length computed as average of all baselines lengths of the network. In this way, the strain rate mainly represents the average deformation pattern of the area (fig. 5) and is poorly sensitive to possible anomalous single vectors (for example the velocity of BUON).

7. Discussion and conclusions

Geological mesostructural data and paleoseismological studies in the Central-Southern Apennines suggest a major change in the stress field in the Middle Pleistocene (Valensise and Pantosti, 1992; Pantosti *et al.*, 1993a; Cinque *et al.*, 1993; Hippolyte *et al.*, 1994, 1995; Valensise and Pantosti, 2001). Due to the relatively young age of the actual stress field (0.6-0.7 Myr), seismic reflection studies do not give a clear evidence of the active structures associated with it, but still show the structures associated with the Apennines mountain building (Mostardini and Merlini, 1986). Active strain and stress estimations, mainly from seismology (Selvaggi and Amato, 1992; Frepoli and Amato, 2000; Viti *et al.*, 2001), breakout in deep wells (Amato and Montone, 1997; Montone *et al.*, 1997), in combination with mesostructural data (Hippolyte *et al.*, 1994, 1995), paleoseismology and quantitative geomorphology (Pantosti and Valensise, 1988; Pantosti *et al.*, 1993a,b; Valensise *et al.*, 1993; Valensise and Pantosti, 2001), indicate a present day NE-SW extension in the Central-Southern Apennines, which seems to be confined to the upper 10-15 km of the crust. The amount of extension is still uncertain because of the different origin, besides the spatial and time intervals of the different geophysical observations.

Westaway (1992), considering instrumental and historical seismicity since 1650 A.D. and assuming widespread normal faulting, estimated an extensional velocity normal to the Central-Southern Apennines as high as 5 mm/yr. Jackson and McKenzie (1988), analyzing the seismicity from 1908 to 1981 for events with magnitude $M_s > 6.0$, found a value of 2.1 mm/yr. Anderson and Jackson (1987) suggest an extension rate of 2.5 mm/yr on the basis of smaller-magnitude events in a shorter period, 21 years. Pondrelli *et al.* (1995) found a lower value, 1.7 mm/yr, using only CMT solutions in the time span 1977-1992. Kiratzi (1994), including all earthquakes from 1870 to 1991, gave an extensional velocity for the Northern-Central Apennines of 3.1 mm/yr. Recently, Selvaggi (1998) gave an extension rate for the Central-Southern Apennines of about 1.6 mm/yr and of 0.3 mm/yr for the Northern Apennines, using historical and recent earthquakes in an interval of 700 years. Bernardini and Gasperini (1994), using 25 earthquakes with $5.5 < M < 7.1$ starting from 1600, obtained extensional velocities ranging from 5.3 mm/yr to 0.7 mm/yr in the area of the GeoModAp network, and a total rate of extension of 2.8 mm/yr for the entire area. The analysis of seismic deformation carried out by Viti *et al.* (2001) implies that the extensional strain rates related to 198 crustal earthquakes, occurred in the period 1915-1998, are roughly 2.5 mm/yr and 4 mm/yr for the Central and Southern Italy respectively. Finally, paleoseismology gives slip rates for the known faults that go from few tenths to 1.4 mm/yr (Valensise and Pantosti, 2001).

Our analysis provides new quantitative information on the present day strain and velocity fields of the studied area, with well-constrained error estimates, which can hardly be assessed by geological and seismological approaches.

As regards the residual velocity field (fig. 4), the most interesting feature is an average NE-ward motion for most of the stations located east and south-east of the Ortona-Roccamonfina tectonic lineament. Among these stations, CAPR, BUON and LUCE show different residual velocity directions. For CAPR, this incoherence could be due to local deformations related to the Campanian volcanism. The motion of LUCE is statistically not significant probably because that during one campaign this station suffered for antenna instability (fig. 3b). Further observations in this station will be performed during repetition campaigns, since this station lye in a suitable area to detect the relative movements between the Apennines and the Apulian foreland. BUON displays a clear anomaly of the residual velocity field not recognized as observation outlier, as exhibited by the time series (fig. 3a). This can be due to local active tectonics or site instabilities, which can be revealed only by a network densification. The stations located on the Apulian platform, MATE, ANGE and TREM, show a coherent residual velocity field, which confirms other evidences on the relative inner stability of this platform, and indicate a different motion trend of this foreland zone with respect to the Central Apennines. The GPS stations located on the chain W and N-W of the Ortona-Roccamonfina lineament show a general N-ward to NW-ward motion. Although the number of stations across this lineament are not enough to allow a detailed and significant estimate of its present kinematics activity, seismic or aseismic, our results seem to confirm the importance of this tectonic lineament as a crustal discontinuity, separating areas with different motions. A more detailed geodynamic interpretation of the kinematics of this zone may be achieved from a rigorous combination of local and regional GPS networks. The processing approach described in this paper may allow us to obtain statistically rigorous solutions even using data derived from networks with different characteristics and observed in different epochs.

More interesting, from a seismotectonic point of view, is the strain rate field that we analyzed following two different approaches. Computing the horizontal strain rate principal axes over a subnetwork of 12 stations (within the dark gray lines of fig. 4) we first estimated the average deformation in this transect of the Apennines (blue arrows in fig. 4), which includes different tectonic domains of the chain. Considering a SW-NE dimension of the GeoModAp network of about 250 km, the mean strain rate value (fig. 4, table VII) gives an extensional velocity of 3.0 ± 0.2 mm/yr, with azimuth $(55 \pm 2)°$, and a significant but lower NNW-SSE compression,

roughly parallel to the chain axis. Then, using a dumped least square interpolation method we detected the spatial trend of the plane strain rate principal axes (black arrows in fig. 5). On the basis of this result, which indicates a transition from N-S compression in the Tyrrhenian side to a NE-SW extension toward the Adriatic, and on the basis of the network geometry, we tentatively subdivided this area into three main subnetworks. From the site velocities of each subnetwork, we computed the principal strain rate axes pertaining to each subnetwork partition (blue arrows in fig. 5, table VII), by solving the over determined least square problem (Feigl *et al.*, 1993). With this approach we obtained in a different way the spatial change of the strain rate field, defining areas with quite homogeneous deformation fields.

On the basis of our data, the interpolated strain rate field shows a minimum along the chain axis, where paleoseismological, geological and macroseismic data identify the main seismogenetic structures. On the contrary, the areas lying outside the chain display higher deformation values. It is worth noting that this result is influenced by the anomalous velocities of BUON and LUCE stations.

Even if this work shows the first well-constrained estimate of extensional velocity in the Central-Southern Apennines from GPS data, it is necessary:

– To densify the GeoModAp geodetic network, to achieve a better resolution of the spatial pattern of deformation styles and to evaluate the present day kinematics of main tectonic structures, as the Ortona-Roccamonfina lineament, or of other minor tectonic lineaments, which may play a major role in controlling the present day strain field.

– To combine the geodetic observations of GeoModAp network with those collected in the Central Mediterranean (using GPS data from permanent, non permanent, local and regional networks and following the same computation approach and) in the frame of the Tyrgeonet project (Anzidei *et al.*, 1995c, 2001), including Northern Africa and Tyrrhenian Sea/Calabrian arc tectonic system, in order to better understand the ongoing deformation of the Apennine chain with respect to a wider area.

The comparison of the geodetic data described in this paper, with the instrumental seismicity data collected in the area during the time span of the geodetic surveys, will provide new insights into the balance between seismic and aseismic deformations and to contribute to the seismic hazard reduction in this seismogenetic area that suffered destructive earthquakes in the last centuries.

Acknowledgements

The authors are grateful to all Agencies, Universities, technicians and single researchers involved during field surveys. Thanks are due to Dr. Z.K. Shen for discussion about strain rate computation and data processing, and to Dr. D. Dong for discussion about velocity adjustment and error analysis. Thanks are also due to Dr. G. Valensise for providing information about paleoseismological data. The maps were created by using the Generic Mapping Tools (GMT) software (Wessel and Smith, 1995). This paper was partially supported by the Italian Space Agency and the EU.

REFERENCES

AMATO, A. and P. MONTONE (1997): Present-day stress field and active tectonics in Southern Peninsular Italy, *Geophys. J. Int.*, **130**, 519-534.

ANDERSON, H.J. and J.A. JACKSON (1987): Active tectonics of the Adriatic region, *Geophys. J. R. Astron Soc.*, **91**, 937-983.

ANZIDEI, M., P. BALDI, G. CASULA, P. ENGLAND, A. GALVANI, S. GANDOLFI, I. HUNSTAD, L. MARGHERITI, F. RIGUZZI and A. ZANUTTA (1995a): Misure GPS nell'ambito del progetto CEE GEOMODAP, in *Atti del XIV Convegno Nazionale del GNGTS*, Roma, Italy, 319-322.

ANZIDEI, M., P. BALDI, G. CASULA, F. RIGUZZI and A. ZANUTTA (1995b): GEOMODAP project GPS network, *Publication of the Istituto Nazionale di Geofisica, Roma*, n. 570, 1-71.

ANZIDEI, M., P. BALDI, G. CASULA, F. RIGUZZI and L. SURACE (1995c): La rete TYRGEONET, *Boll. Geod. Sci. Affini, Special Supplement*, **LIV** (2), 1-19.

ANZIDEI, M., P. BALDI, G. CASULA, A. GALVANI, E. MANTOVANI, A. PESCI, F. RIGUZZI and E. SERPELLONI (2001): Insights on present-day crustal motion in the Central Mediterranean area from GPS surveys, *Geophys. J. Int.*, **146** (1), 98-110.

BALDI, P., E. DEGLI ANGELI, L. PIALLINI and E. MANTOVANI (1982): Gravity anomaly interpretation in the Cala-

brian Arc and surrounding regions: a tridimensional approach, *Earth Evol. Sci.*, **3**, 243-247.

BERNARDINI, F. and P. GASPERINI (1994): Tassi di deformazione cosismica nell'Appennino centro-meridionale sulla base di informazioni macrosismiche, in *Atti del XIII Convegno Nazionale del GNGTS*, Roma, 815-826.

BOSCHI, E., G. FERRARI, P. GASPERINI, E. GUIDOBONI, G. SMRIGLIO and G. VALENSISE (1995): *Catalogo dei Forti Terremoti in Italia dal 461 a.C. al 1980* (ING, Roma - SGA, Bologna), pp. 973 and CD-ROM.

BOSCHI, E., E. GUIDOBONI, G. FERRARI, G. VALENSISE and P. GASPERINI (1997): *Catalogo dei Forti Terremoti in Italia dal 461 a.C. al 1990* (ING, Roma - SGA, Bologna), pp. 644 and CD-ROM.

BOSCHI, E., D. GIARDINI, D. PANTOSTI, G. VALENSISE, R. ARROWSMITH, P. BASHAM, R. BURGMANN, A. CRONE, A. HULL, R. MCGUIRE, D. SCHWARTZ, K. SIEH, S. WARD and R. YEATS (1998): New trends in active faulting studies for seismic hazard assessment, *Ann. Geofis.*, **39** (6), 1301-1307.

BOSCHI, E., E. GUIDOBONI, G. FERRARI, D. MARIOTTI, G. VALENSISE and P. GASPERINI (2000): Catalogo dei forti terremoti in Italia 461 a.C. -1997, *Ann. Geofis.*, **43** (4), 609-868 and CD-ROM.

CASSINIS, R., R. FRANCIOSI and S. SCARASCIA (1979): The structure of the Earth's crust in Italy: a preliminary typology based on seismic data, *Boll. Geofis. Teor. Appl.*, **21**, 105-126.

CASTELLARIN, A., R. COLACICCHI, A. PRATURLON and C. CANTELLI (1982): The Jurassic-Lower Pliocene history of the Ancona-Anzio line (Central Italy), *Mem. Soc. Geol. It.*, **24**, 325-336.

CHIARABBA, C. and A. AMATO (1997): Crustal velocity structure of the Apennines (Italy) from *P*-wave travel time tomography, *Ann. Geofis.*, **39** (6), 1133-1148.

CINQUE, A., E. PATACCA, P. SCANDONE and M. TOZZI (1993): Quaternary kinematic evolution of the Southern Apennines. Relationships between surface geological features and deep lithospheric structures, *Ann. Geofis.*, **36** (2), 249-260.

COCCO, M., G. SELVAGGI, M. DI BONA and A. BASILI (1993): Recent seismic activity and earthquake occurrence along the Appennines, in *Recent Evolution and Seismicity of the Mediterranean Region*, edited by E. BOSCHI, E. MANTOVANI and A. MORELLI (Kluwer Academic Publishers, The Netherlands), 295-312.

DEMETS, C., G. GORDON, D.F. ARGUS and S. STEIN (1994): Effect of recent revisions to the geomagnetic reversal time scale on estimates of current plate motions, *Geophys. Res. Lett.*, **21**, 2191-2194.

DEWEY, J.F., M.L. HELMAN, E. TURCO, D.H.W. HUTTON and S.D. KNOTT (1989): Kinematics of the Western Mediterranean, in *Alpine Tectonics*, edited by M.P. COWARD and D. DIETRICH, *Geol. Soc. Spec. Publ.*, **45**, 265-283.

DONG, D. and Y. BOCK (1989): Global positioning system analysis with phase ambiguity resolution applied to crustal deformation studies in California, *J. Geophys. Res.*, **94**, 3949-3966.

DONG, D., T.A. HERRING and R.W. KING (1998): Estimating regional deformation from a combination of space and terrestrial geodetic data, *J. Geophys. Res.*, **72**, 200-214.

FEIGL, K.L., R.W. KING and T.H. JORDAN (1990): Geodetic measurement of tectonic deformation in the Santa Maria fold and thrust belt, California, *J. Geophys. Res.*, **90**, 2679-2699.

FEIGL, K.L., D.C. AGNEW, Y. BOCK, D. DONG, A. DONNELLAN, B.H. HAGER, T.A. HERRING, D.D. JACKSON, T.H. JORDAN, B.W. KING, S. LARSEN, K.M. LARSON, M.H. MURRAY, Z.K. SHEN and F.H. WEBB (1993): Space geodetic measurements of crustal deformation in Central and Southern California, 1984-1992, *J. Geophys. Res.*, **98**, 21677-21712.

FREPOLI, A. and A. AMATO (2000): Fault plane solutions of crustal earthquakes in Southern Italy (1988-1995): seismotectonic implications, *Ann. Geofis.*, **43** (3), 437-467.

FREPOLI, A., G. SELVAGGI, C. CHIARABBA and A. AMATO (1996): State of stress in the Southern Tyrrhenian subduction zone from fault-plane solutions, *Geophys. J. Int.*, **125**, 879-891.

GASPARINI, C., G. IANNACONE and R. SCARPA (1985): Fault plane solutions and seismicity of the Italian Peninsula, *Tectonophysics*, **117**, 59-78.

GASPERINI, P., F. BERNARDINI, G. VALENSISE and E. BOSCHI (1999): Defining seismogenic sources from historical earthquake felt report, *Bull. Seismol. Soc. Am.*, **84**, 94-110.

GEISS, E. (1987): A new compilation of crustal thickness data for the Mediterranean area, *Ann. Geophys., Ser. B*, **5**, 623-630.

GIESE, P. and C. MORELLI (1975): Crustal structure in Italy, in *Structural Model of Italy*, edited by L. OGNIBEN *et al.*, CNR, *Quad. Ric. Sci.*, **90**, 453-489.

HERRING, T.A. (1999): GLOBK: *Global Kalman filter VLBI and GPS Analysis Program*, version 5.0, Mass. Inst. of Techn., Cambridge.

HIPPOLYTE, J.C., J. ANGELIER and F. ROURE (1994): A major geodynamic change revealed by Quaternary stress patterns in the Southern Appennines (Italy), *Tectonophysics*, **240**, 199-210.

HIPPOLYTE, J.C., J. ANGELIER and E. BARRIER (1995): Compressional and extensional tectonics in an arc system: example of the Southern Apennines, *J. Struct. Geol.*, **17**, 1725-1740.

HUNSTAD, I. and P. ENGLAND (1999): An upper bound on strain in the Central Apennines, Italy, from triangulation measurements between 1869-1963, *Earth Planet. Sci. Lett.*, **169**, 261-267.

JACKSON, J. and D. MCKENZIE (1988): The relationship between plate motion and seismic moment tensor, and the rates of active deformation in the Mediterranean and Middle East, *Geophys. J. Int.*, **93**, 45-73.

KING, R.W. and Y. BOCK (1995): *Documentation for the MIKT GPS Analysis Software: GAMIT*, version 10.01, Mass. Inst. of Techn., Cambridge.

KIRATZI, A.A. (1994): Active seismic deformation in the Italian Peninsula and Sicily, *Ann. Geofis.*, **37** (1), 27-45.

LUCENTE, F.P., C. CHIARABBA, G.B. CIMINI and D. GIARDINI (1999): Tomographic constraints on the geodynamic evolution of the Italian region, *J. Geophys. Res.*, **104**, 20307-20327.

MALVERN, L.E. (1969): *Introduction to Mechanics of a Continuous Medium*, Prentice, New Jersey.

MANTOVANI, E., D. ALBARELLO, C. TAMBURELLI, D. BABBUCCI and M. VITI (1997a): Plate convergence, crustal delamination, extrusion tectonics and minimization of shortening work as main controlling factors of the recent Mediterranean deformation pattern, *Ann. Geofis.*, **40** (3), 611-643.

MANTOVANI, E., D. ALBARELLO, D. BABBUCCI and C. TAMBURELLI (1997b): Recent/present tectonic processes in the Italian region and their relation with seismic and volcanic activity, *Ann. Tectonicae*, **13** (1-2), 27-57.

MANTOVANI, E., D. ALBARELLO, D. BABBUCCI, C. TAMBURELLI and M. VITI (2000a): Generic mechanism of back arc opening: insights from the Mediterranean deformation pattern, in *Problems in Geophysics for the New Millenium*, edited by E. BOSCHI, G. EKSTRÖM and A. MORELLI, 151-178.

MANTOVANI, E., M. VITI, D. ALBARELLO, C. TAMBURELLI, D. BABBUCCI and N. CENNI (2000b): Role of kinematically induced forces in Mediterranean tectonics: insights from numerical modelling, *J. Geodyn.*, **30** (3), 287-320.

MAO, A., C.G.A. HARRISON and T.H. DIXON (1999): Noise in GPS coordinate time series, *J. Geophys. Res.*, **104**, 2797-2816.

MONTONE, P., A. AMATO, A. FREPOLI, M.T. MARIUCCI and M. CESARO (1997): Crustal stress regime in Italy, *Ann. Geofis.*, **40** (3), 741-757.

MOSTARDINI, F. and S. MERLINI (1986): Appennino centro meridionale – Sezioni geologiche e proposta di modello strutturale, *Mem. Soc. Geol. It.*, **35**, 177-202.

NICOLICH, R. (1989): Crustal structures from seismic studies in the frame of the European Geotraverse (southern segment) and crop projects, in *The Lithosphere in Italy, Advances in Earth Science Research*, edited by A. BORIANI, M. BONAFEDE, G.B. PICCARDO and G.B. VAI, Acc. Naz. Lincei, Roma, pp. 540.

ORAL, M.B. (1994): Global Positioning System (GPS) measurements in Turkey (1988-1992): kinematics of the Africa-Arabia-Eurasia plate collision zone, *Ph.D. Thesis*, Mass Inst. of Techn., Cambridge.

PANTOSTI, D. and G. VALENSISE (1988): La faglia sud-appenninica: identificazione oggettiva di un lineamento sismogenetico nell'Appennino meridionale, in *Atti del VII Convegno Nazionale del GNGTS*, Roma, 205-220.

PANTOSTI, D., D.P. SCHWARTZ and G. VALENSISE (1993a): Paleoseismology along the 1980 surface rupture of the Irpinia fault: implications for earthquake recurrence in the Southern Appennines, Italy, *J. Geophys. Res.*, **98**, 6561-6577.

PANTOSTI, D., G. D'ADDEZIO and F.R. CINTI (1993b): Late Holocene surface faulting earthquakes on the Ovindoli-Pezza Fault (OPF)-Central Italy, *Terra abstracts*, suppl. n. 1, *Terra Nova*, **5**, 265.

PATACCA, E. and P. SCANDONE (1989): Post-Tortonian mountain building in the Apennines: the role of the passive sinking of a relict lithospheric slab, in *The Lithosphere in Italy: Advances in Earth Science Research*, edidet by A. BORIANI, M. BONAFEDE, G.B. PICCARDO and G.B. VAI, Acc. Naz. Lincei, Roma, **80**, 157-176.

PATACCA, E., R. SARTORI and P. SCANDONE (1990): Tyrrhenian basin and Apenninic arcs: kinematic relations since Late Tortonian times, *Mem. Soc. Geol. Ital.*, **45**, 425-451.

PHILIP, H. (1987): Plio-Quaternary evolution of the stress field in Mediterranean zones of subduction and collision, *Ann. Geophys.*, **5B** (3), 301-320.

PONDRELLI, S., A. MORELLI and E. BOSCHI (1995): Seismic deformation in the Mediterranean area estimated by Moment Tensor Summation, *Geophys. J. Int.*, **122**, 938-952.

ROEDER, D. (1984): Tectonic evolution of the Apennines, *Am. Ass. Petrol. Geol. Bull.*, **68**, 798.

ROTHACHER, M. and G. MADER (1996): Combination of antenna phase centre offsets and variations: antenna calibration set IGS_1, *anonymous ftp ubeclu.unibe.ch*, June, 1996.

ROTHACHER, M., W. GURTNER, S. SCHAER, R. WEBWER and H.O. HASE (1996): Azimuth and elevation dependent phase center corrections for geodetic GPS Antennas Estimated from GPS calibration campaigns, *in IAG Symposium*, edited by W. TORGE (Springer-Verlag), No. 115, 335-339.

ROURE, F., P. CASERO and R. VIALLY (1991): Growth processes and melange formation in the Southern Apennines accretionary wedge, *Earth Planet. Sci. Lett.*, **102**, 395-412.

SAASTAMOINEN, J. (1972): Atmospheric correction for the troposphere in radio ranging of satellites. In the use of artificial satellites for Geodesy, *Geophys. Monogr. Ser.*, **15**, Am. Geophys. Un., Washington, D.C.

SELVAGGI, G. (1998): Spatial distribution of horizontal seismic strain in the Apennines from historical earthquakes, *Ann. Geofis.*, **41** (2), 241-251.

SELVAGGI, G. and A. AMATO (1992): Subcrustal earthquakes in the Northern Apennines (Italy): evidence for a still active subduction?, *Geophy. Res. Lett.*, **19** (21), 2127-2130.

SELVAGGI, G., B. CASTELLO and R. AZZARA (1997): Spatial distribution of scalar moment release in Italy (1983-1996): seismotectonic implications for the Apennines, *Ann. Geofis.*, **40** (6), 1565-1578.

SERRI, G.F., F. INNOCENTI and P. MANETTI (1993): Geochemical and petrological evidence of the subduction of delaminated Adriatic continental lithosphere in the genesis of the Neogene-Quaternary magmatism of Central Italy, *Tectonophysics*, **223**, 117-147.

SHAFFRIN, B. and Y. BOCK (1988): A unified scheme for processing GPS phase observations, *Bull. Geod.*, **62**, 142-160.

SHEN, Z.K., D.D. JACKSON and B.X. GE (1996): Crustal deformation across and beyond the Los Angeles basin from geodetic measurements, *J. Geophys. Res.*, **101**, 27957-27980.

SHEN, Z.K., C. ZHAO, A. YIN, Y. LI, D.D. JACKSON, P. FANG and D. DONG (2000): Contemporary crustal deformation in East Asia constrained by Global Positioning System measurements, *J. Geophys. Res.*, **105**, 5721-5734.

SURACE, L. (1997): La nuova rete geodetica nazionale IGM95: risultati e prospettive di utilizzazione, *Boll. Geod. Sci. Affini*, **3**, 357-377.

VALENSISE, G. and D. PANTOSTI (Editors) (2000): Database of potential sources for earthquakes larger than *M* 5.5 in Italy, Release 1.0, July 2000, to appear in *Quaderni di Geofisica*.

VALENSISE, G. and D. PANTOSTI (2001): The investigation of potential earthquake sources in peninsular Italy: a review, *J. Seismol.*, **5**, 287-306.

VALENSISE, G., D. PANTOSTI, G. D'ADDEZIO, F.R. CINTI and L. CUCCI (1993): L'identificazione e la caratterizzazione di faglie sismogenetiche nell'Appennino centro-meridionale e nell'arco Calabro: nuovi risultati ed ipotesi interpretative, in *Atti del XII Convegno GNGTS, CNR*, Roma, Novembre 1993, 331-342.

VESPE, F., G. BIANCO, M. FERMI, C. FERRARO, A. NARDI and C. SCIARRETTA (2000): The Italian GPS fiducial network: services and products, *J. Geodyn.*, **30**, 327-336.

VITI, M., D. ALBARELLO and E. MANTOVANI (2001): Classification of seismic strain estimates in the Mediterranean region from a bootstrap approach, *Geophys. J. Int.*, **146** (2), 399-415.

WARD, S.N. (1994a): A multidisciplinary approach to seismic hazard in Southern California, *Bull. Seismol. Soc. Am.*, **84**, 1293-1309.

WARD, S.N. (1994b): Constraints on the seismotectonics of the Central Mediterranean from Very Long Baseline Interferometry, *Geophys. J. Int.*, **117**, 441-452.

WESSEL, P. and W.H.F. SMITH (1995): *The Generic Mapping Tools (GMT) version 3.0*, Technical Reference and Cookbook, SOEST/NOAA.

WESTAWAY, R. (1992): Seismic moment summation for historical earthquakes in Italy: tectonic implications, *J. Geophys. Res.*, **97**, 15437-15464.

ZHANG, J. (1996): Continuous GPS measurements of crustal deformation in Southern California, *Ph.D. dissertation*, Univ. of Calif., San Diego.

ZHANG, J., Y. BOCK, H. JOHNSON, P. FANG, S. WILLIAMS, J. GENRICH, S. WDOWINSKI and J. BHER (1997): Error analysis of daily position estimates and site velocities, *J. Geophys. Res.*, **102**, 18035-18055.

(received March 12, 2001;
accepted May 21, 2001)